PHYSICAL REVIEW B VOLUME 25, NUMBER 2 15 JANUARY 1982

Charge-density-wave motion in $NbSe_3$. I. Studies of the differential resistance dV/dI

P. Monceau, J. Richard, and M. Renard
Centre de Recherches sur les Très Basses Températures, Centre National de la Recherche Scientifique, B. P. 166 X, 38042 Grenoble-Cedex, France
(Received 4 May 1981)

We have measured the variation of the differential resistance as a function of the electric field for temperatures below those at which the two charge-density waves (CDW) form in $NbSe_3$. The shape of the dV/dI variation is very sensitive to temperature, particularly below that at which the anomaly due to the lower CDW shows its maximum. We have observed that for some samples a very sharp drop with a deep minimum in dV/dI occurs at the critical electric field value where the charge-density wave is depinned. Over a large range of electric field below this dip we have measured low-frequency noise. We develop a model where the phase of the charge-density wave is described as an overdamped oscillator. If we consider the sample as consisting of a unique domain, we find that the differential resistance has an infinite negative value at the critical electric field when the current in the sample is regulated. We also obtain expressions for the variation of the frequency of the modulation of the current carried by the charge-density wave as a function of the electric field and for the amplitudes of the harmonics of this modulated current. To account for a more realistic description of the sample we suppose that it is formed of multiple domains. We explain the low-frequency noise as the depinning of individual domains and the dip in dV/dI as resulting from the distribution of the electric critical fields of this assembly of domains. We have also studied the dV/dI variation for $NbSe_3$ samples doped with tantalum and titanium. The shape of the dV/dI variation near the critical field gives a good indication of the distribution of the pinning centers inside the sample.

I. INTRODUCTION

Among the transition-metal trichalcogenides, $NbSe_3$ has been the most intensively studied since 1975 (when it was synthesized for the first time[1]) because of its many interesting properties. Two charge-density waves (CDW's) occur at $T_1 = 145$ K and $T_2 = 59$ K.[2] Superstructures have been observed by electron diffraction[3–5] and x-ray studies.[6] The CDW's are incommensurate with the main lattice, and the wave vectors along the a^*, b^*, and c^* directions are, respectively, (0,0.243,0) at T_1 and (0.5,0.259,0.5) at T_2. The two CDW's seem to be independent, as can be seen by the absence of variation in the intensities of the superlattice spots of the upper transition at the temperature where the lower one develops.[6] Interplay between CDW distortions and superconductivity is very sensitive to pressure or impurities. Pressure studies indicate that T_2 decreases rapidly with pressure and has disappeared for $P \sim 5.5$ kbar.[7] Above this pressure $NbSe_3$ is a bulk anisotropic superconductor with a total Meissner effect[8] and a ratio of 5.5 between the superconducting critical fields when H is parallel or perpendicular to the chain direction.[9] Zero resistivity below 1.5 K has been measured on samples doped with titanium,[10] zirconium,[11] and tantalum[12] impurities. Magnetoresistance measurements at low temperature reveal periodic oscillations and the mapping of the Fermi surface which remains after the two successive lattice distortions have been made.[13,14] The fect of the pressure on the shape of the Fermi surface at low temperature has also been studied.[8]

However, the more fascinating properties of $NbSe_3$ are related to nonlinearity induced by the electric field below T_1. It was shown that the resistive anomalies associated with the gap formation below T_1 and T_2 were strongly reduced with weak dc electric fields [a few tenths of V/cm for T_1 and typically 1 V/cm for T_2 (Ref. 15)] and were frequency dependent.[16,17] The extra conduc-

tivity was interpreted as the conductivity associated with the motion of the CDW's.[18] Fröhlich[19] in 1954 proposed a model where a CDW could slide freely in the crystal without resistance if its phase were invariant by translation in the crystal. Lee, Rice, and Anderson[20] showed that, in reality, the phase of the CDW could be pinned by several mechanisms, such as commensurability between the main lattice and the period of the CDW or Coulomb interactions between adjacent chains or impurity pinning. However, if an electric field strong enough to overcome the pinning energy were applied, the CDW can be depinned and carries a current. This depinning field E_c was calculated by Lee and Rice[21] and observed by Fleming and Grimes.[22] This field is impurity dependent. Several laws have been calculated by Lee and Rice[21] according to the type of impurities: a parabolic dependence on the impurity concentration for isoelectronic impurities or a linear dependence for nonisoelectronic ones. Experimentally, it has been shown that E_{c1} [for T_1 (Ref. 23)] and E_{c2} [for T_2 (Refs. 10 and 24)] increase with the amount of impurities.

Lee and Rice[21] suggested that the motion of the CDW could be a motion as a whole or through dislocations generated inside the CDW superlattice by, for instance, Franck-Read sources. The extra conductivity was also explained by the creation of soliton-antisoliton pairs by the electric field[25] or by the depinning and the motion of soliton lattices.[26] Finally, the non-Ohmic conductivity was associated by Bardeen[27] with the tunneling of the CDW through the pinning potential. Introduction of a correlation length in this theory[28] leads to a critical electric field.

At the same electric field where nonlinearity starts, Fleming and Grimes[22] observed that noise was generated between the voltage leads of the samples. A study of this noise showed that it was formed of two parts: a broad-band noise and a quasiperiodic noise,[22,29–31] whose frequencies increase with the electric field. We applied a rf field to $NbSe_3$ samples in the nonlinear state, and we showed that interferences between the external frequency and the periodic noise occurred. These interferences were seen as steps in the dc $I(V)$ characteristics.[32] We interpreted the periodic noise as the Fourier spectrum of the motion of the CDW in the anharmonic potential created by the impurities.[32] We verified the proportionality between the current carried by the CDW and the velocity of the wave.

Hereafter, we report measurements of differential resistivity, noise analysis, and synchronization with external rf fields for the two CDW's of several samples of $NbSe_3$ with different purities. We organize our results in a series of two papers as follows: In paper I we discuss the differential resistivity dV/dI as a function of the applied current. We show that for some temperatures and for some samples dV/dI has a sharp dip near the critical field. We calculate the $V(I)$ characteristic with the model we used previously[32] and show that if the sample is considered as a single oscillator the model cannot account for the experimental results. In fact, Fung and Steeds[33] have observed in $NbSe_3$ by dark-field electron-microscope studies domains whose typical dimensions are 2 μm$\times$200 Å$\times$200 Å. Assuming a Gaussian distribution of critical electric fields for the multiple domains, we can explain qualitatively the dV/dI variation.

In paper II we concentrate on the quasiperiodic noise. We have performed synchronization of the noise frequencies by external rf field for the two CDW's. We show that the proportionality between the current carried by the CDW and the velocity is the same for each CDW. We conclude that the numbers of electrons carried by the wave is the same for the two CDW's. We generalize our previous work where a unique domain radiated a rf current. With a multidomain assembly we show that all the frequencies generated in each domain self-synchronize to give a coherent signal across the sample.

II. EXPERIMENTAL TECHNIQUES

The $NbSe_3$ crystals were grown as described in Ref. 1. We recall that its structure consists of infinite chains of selenium trigonal prisms stacked on top of each other by sharing the triangular faces. The niobium atoms are located roughly at the center of the prisms. The chains are parallel to the b axis, and the chains are linked together so as to form infinite slabs parallel to the bc plane. These slabs are two trigonal prisms thick and they are linked together by weak Se—Se bonds. Band-structure[34,35] studies show that the energy bands rise rapidly along the b axis but vary slowly along the directions perpendicular to the chain axis, indicating a pseudo-one-dimensional character for $NbSe_3$. These calculations also show the Fermi level crosses only four bands.

The monoclinic unit cell is formed with six chains which, following Wilson,[36] can be separated

in three groups of two according to the distance between the Se—Se bondings in the basic triangle of each trigonal prism. These distances are, respectively, 2.37, 2.49, and 2.91 Å. The two short distances are of the same order of magnitude as that found in solid selenium (2.32 Å) and suggest a covalent bonding Se_2^{2-}. The six cations per unit cell introduce 30 electrons. Each chain with strong interaction Se-Se ($\times 4$) accounts for two electrons for Se_2^{2-} and two electrons for Se^{2-}. The chain with the weakest Se-Se interaction ($\times 2$) accounts for 2×3 electrons for each Se^{2-}. Two electrons remain to be shared between only four niobium atoms (because the energy band of the chains with an equilateral basis is much higher than the Fermi level[34–36]). Thus there are 0.5 electron per niobium; with the spin degeneracy the Fermi level in the one-dimensional picture is exactly at $0.25b^*$. In fact, the four niobium atoms are not exactly equivalent and there are not exactly 0.5 electron per each niobium; experimentally, the superstructure spots appear at $0.243b^*$ for T_1 and $0.259b^*$ for T_2.

The previous measurements gave an absolute resistivity of 600 $\mu\Omega$ cm.[16] Because of the great difficulty of measuring accurately the cross-section area, values of the absolute resistivity show great dispersion in the literature. We measured the cross section of several crystals with a scanning electron microscope and found $\rho \sim 250$ $\mu\Omega$ cm.[32] Ong and Gould[31] have reported $\rho \sim 150$ $\mu\Omega$ cm, Nakamura and Aoki[37] a value of 100 $\mu\Omega$ cm, and Kahlert[38] a even smaller value on a very tiny sample (~ 1 μm^2). In the following we will keep the value of 250 $\mu\Omega$ cm, but a large uncertainty remains which requires more systematic measurements.

With two electrons for each unit cell we obtain at room temperature an electron concentration of 3.9×10^{21} cm^{-3}. Tessema and Ong[39] have deduced from Hall-effect measurements a value of 1.39×10^{21} cm^{-3}, which is less than 3 times lower than the value we obtained. We think that the description of $NbSe_3$ as a semimetal with small pockets of holes and electrons is not correct at room temperature.[36] Such a model requires that some bands cross near the Fermi level as for tetrathiafulvalene tetracyanoquinodimethane (TTF-TCNQ) where the bands are π type. However, in $NbSe_3$ all the bands are dz^2 type, and band calculations show that their energies monotonically increase along the b axis.

It is interesting to compare $NbSe_3$, for example, to copper. The conductivity is given by $\sigma = ne^2\tau/m^*$; for copper m^* equals the electronic mass m and $n \sim 25\,000$ C/cm^3. For $NbSe_3$ $m^* \sim 6m$ (the effective mass of the d electrons of niobium) and we estimate $n \sim 625$ C/cm^3 (with two electrons per unit cell). So

$$\frac{\sigma_{Cu}}{\sigma_{NbSe_3}} \sim 250 \frac{\tau_{Cu}}{\tau_{NbSe_3}}$$

but $\sigma_{Cu} = 62.5\times 10^4$ $(\Omega\,\text{cm})^{-1}$ and we take $\sigma_{NbSe_3} = 0.4\times 10^4$ $(\Omega\,\text{cm})^{-1}$ and

$$\frac{\sigma_{Cu}}{\sigma_{NbSe_3}} \sim 150 \, .$$

Unfortunately we do not know τ_{NbSe_3}. It is likely that in a covalo-ionic system as $NbSe_3$, it might be lower than that in copper. However, by this comparison we show that the number of electrons at room temperature for $NbSe_3$ can be deduced by simple calculations.

We have performed experiments on many samples from different batches. We report results on seven samples. In Table I we indicate the resistance ratio between room temperature and helium temperature, the length of the samples, the critical fields E_{c1} and E_{c2} at the temperatures where the resistance is maximum (125 K for E_{c_1} and 47 K for E_{c_2}).

The differential resistance of the samples is measured with four contacts by an ac bridge working at a frequency of 33 Hz. Its bandpass width is $1/4\tau$, where τ is the time constant of the filter behind the lock-in detector (typically 0.3 or 1 s). The noise factor is 0.6×10^{-9} $V/\sqrt{Hz}$. The ac current can be varied between 0.01 and 10 μA. Superposed on this ac current we sweep linearly with time a dc current, and we record the output of the bridge as a function of this dc current on an x-y recorder. After many temperature cyclings and high dc current excursions, we have observed that contacts made by pressure between the sample and gold leads evaporated on a quartz substrate always give the same variation of dV/dI for the two orientations of I whereas silver paint contacts deteriorated faster. The contacts of sample 5 were made with silver paint and those of sample 6 by pressure.

The samples were inserted in a regulated helium-gas flow, and the temperature was measured with calibrated germanium and platinum thermometers near the sample. The stabilization of the temperature was better than 0.1 K for

TABLE I. Lengths, residual resistance ratio (RRR), and critical electric fields E_{c_1} and E_{c_2} at the temperatures where the resistance is maximum (125 K for E_{c_1} and 47 K for E_{c_2}) for all the samples studied in this work. We indicate also the kind of noise analysis performed on these samples: analysis with a spectrum analyzer or with synchronization with an external frequency. (Sample 1 was labeled as sample $B2$ of Ref. 32.)

$NbSe_3$ sample		l (mm)	Room temperature resistance (Ω)	RRR	E_{c_1} (mV/cm)	E_{c_2} (mV/cm)	Spectrum analyzer	Frequency synchronization	Batches
	1	1.0	153	97.8		58.6	32 K $< T <$ 52 K	$T=47$ K	A
	2	0.6	114	17.6		100	$T=47$ K	$T=47$ K	B
	3	1.0	21.6	17.3		54		$T=41$, 46, and 52 K	C
	4	0.35	127	38.7	395	87			A
	5	0.85	93	22.3	395	50		35 K $< T <$ 53 K 99 K $< T <$ 135 K	C
	6	1.25	329	22.4		40	$T=36$, 49, and 54 K	$T=49$ K	C
doped with 250 ppm of Ta	7	0.625	210	7.3	1471	433		$T=40$ and 46 K	D
doped with 1000 ppm of Ti	8	0.95	541	7.2		376			E

several hours. For temperatures below the peak in resistivity, any heating of the sample is easily detected because dV/dI increases before the decrease due to the depinning of the CDW. Such heating is important for the T_1 transition because of the large value of the depinning fields. Consequently, we have immersed the samples in liquid argon. Argon gas is condensed at 87 K at ambient pressure. The temperature can be varied between the critical point at 150.9 K under 48.3 bars and the triple point at 83.8 K for 0.6 bar. The indication of temperature was given by the calibration of the vapor pressure of argon but, because of possible temperature stratification, the temperature was measured with a platinum thermometer near the sample. Typically in the range of temperature where we performed experiments the maximum dissipation in the sample was 0.1 W/cm^2. The heat exchange between the sample and the liquid argon is expected to be very satisfactory up to 1 W/cm^2.

For measuring the noise the voltage across the sample was amplified with a differential preamplifier PAR 116 connected to a PAR 124A lock-in amplifier used as an ac voltmeter. We have recorded the noise as a function of the applied current either with a broad-band frequency facility or for some well-defined frequencies with the selective facility typically with a quality factor Q of 20. The ac voltmeter gives only an rms value if the signal is sinusoidal, which is probably the case for the selective measurements but not exactly true for the broad-band measurements.

III. EXPERIMENTAL RESULTS

A. Temperature dependence of dV/dI

In Fig. 1 we show the variation of dV/dI for sample 4 as a function of the applied current for different temperatures below T_2. As found previously by Fleming and Grimes[22] the differential resistance is constant up to a critical current [as for all our measurements we regulate the current, so we use either the critical electric field E_c or the critical current $I_c=(l/R)E_c$] above which it decreases and where noise (in this experiment at 33 Hz) is generated in the sample. For sample 4 the minimum of the critical field E_{c_2} is 87 mV/cm at 45.5 K. E_{c_2} increases at low temperature and also near T_{c_2}. We observed the same variation of dV/dI with temperature for sample 1 (labeled B2 in Ref. 32).

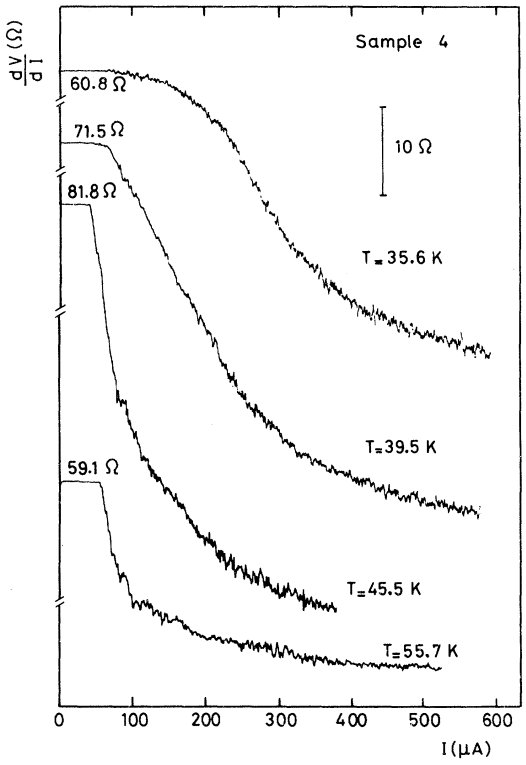

FIG. 1. Variation of the differential resistance dV/dI as a function of the applied current for different temperatures for sample 4. The sharp drop in dV/dI defines the depinning electric field of the CDW.

When the nonlinear properties of $NbSe_3$ were discovered for the first time,[15] it was found that experimentally the conductivity followed the expression

$$\sigma=\sigma_a+\sigma_b e^{-E_0/E}, \tag{1}$$

suggesting a Zener tunneling. To account for the critical field Fleming and Grimes[22] postulated that the total current was given by $J=\sigma' E$ with

$$\sigma'(E)=\begin{cases}\sigma_a & \text{for } E<E_c \\ \sigma_a+\sigma_b e^{-E_0'/(E-E_c)} & \text{for } E>E_c\end{cases}. \tag{2}$$

Recently Fleming[29] proposed another empirical expression for the conductivity:

$$\sigma=\begin{cases}\sigma_a & \text{for } E<E_c \\ \sigma_a+\dfrac{E-E_c}{E}\sigma_b e^{-E_0/(E-E_c)} & \text{for } E>E_c\end{cases}. \tag{3}$$

The differential conductivity obtained from expressions (2) and (3) can be calculated with three parameters: E_0, E_c, and σ_b/σ_a. A good agreement was found by Fleming and Grimes[22] and Fleming,[29] although structures in the variation of dV/dI as a function of E lead to small deviations between experimental and calculated variations.

For sample 4 the dV/dI variation at 55.7 K is very similar to the measurement reported by Fleming for approximately the same temperature. The extra conductivity is nearly saturated above $3E_c$. However, when T is decreased the variations of dV/dI do not follow expressions (2) or (3). A decrease in dV/dI is still observed up to $8E_c$. At low temperature dV/dI shows a large rounding near the critical field.

We have observed new features in the variation of dV/dI and we show in Fig. 2 the results for sample 5. For the upper CDW transition (at $T=130.9$ K) and near T_2 (for $T=54.4$ K) dV/dI follows the same behaviour as sample 4 and is similar to the Fleming results. But when T decreases typically below 52 K, the variation of dV/dI can be separated into four parts according to the strength of the electric field. At low current dV/dI is constant without any noise; after that a slight decrease of dV/dI (less than 10^{-2} of the low field resistance) is observed with a very small low-frequency noise (33 Hz in this experiment); then dV/dI shows a very sharp drop with a minimum in an electric-field range of a few percent of the critical field; for higher electric fields dV/dI decreases slowly with the current. This kind of behavior was obtained for many samples of different batches. The sharp dip cannot be related to the purity of the sample. Sample 4 with a resistance ratio of 38 does not show this dip, whereas sample 5 with a resistance ratio of 22.3 does. However, the samples doped with titanium or tantalum have a variation of dV/dI with the current, similar to sample 4. In Fig. 3 we have drawn the dV/dI variation for a sample doped with 1000 ppm of titanium (sample 8). The sample was grown in a batch with niobium and selenium in stochiometric proportions and with 1000 ppm of titanium. We do not know the exact amount of impurities in the sample because different samples from the same batch do not have the same resistance ratio. Sample 8 has a resistance ratio of 7.2. At 49.2 and 45.9 K a well-defined critical field is measured. However at 40.3 K, before the decrease of dV/dI, there is a electric-field range where noise is observed without variation of dV/dI. This

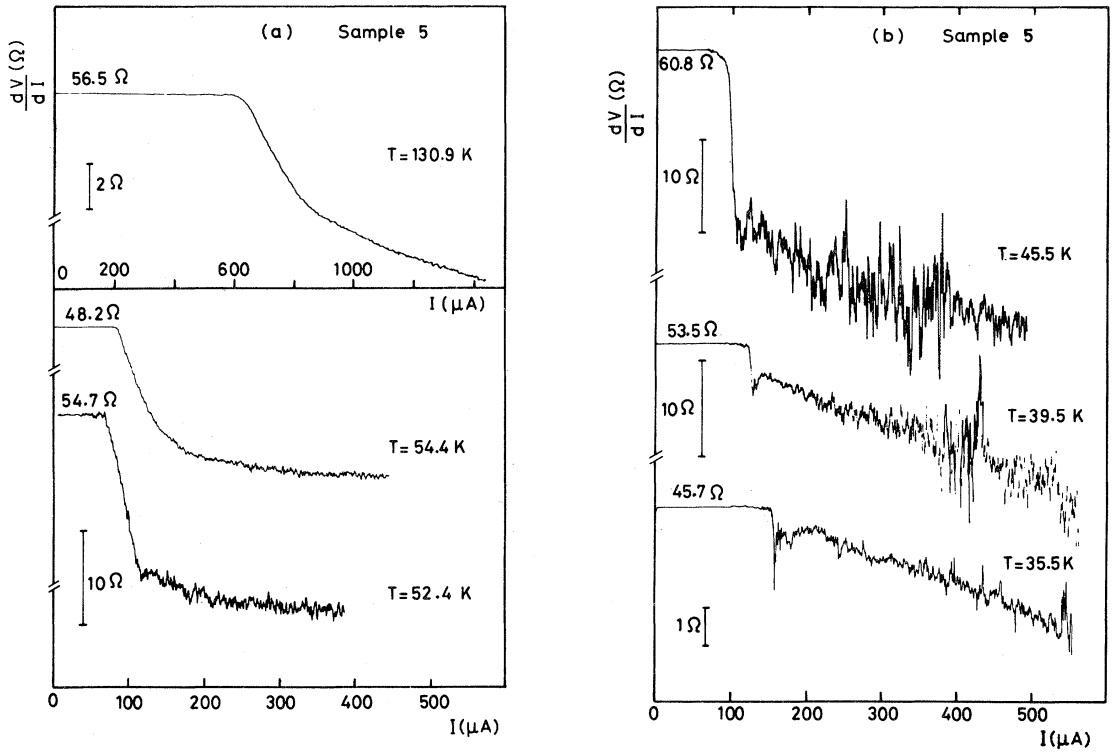

FIG. 2. Variation of the differential resistance dV/dI as a function of the applied current for sample 5. The curve at 130.9 K corresponds to the depinning to the upper CDW transition. The other curves concern the lower CDW. The shape of the variation of dV/dI at low temperature is totally different when compared with sample 4 shown in Fig. 1. A sharp dip in dV/dI is observed below 45.5 K.

electric-field range increases when T decreases, But for this very impure sample we do not observe sharp dips as for sample 5. We measured typically the same variation for a $NbSe_3$ doped with tantalum with the same resistance ratio.

A comment has to be made here about the critical electric field as a function of the purity of the samples. In Table I we report the critical electric fields at the temperature where they are minimum for the T_2 transition. It is clear that E_c increases when impurities are introduced. However, tantalum is believed to be an isoelectronic impurity and consequently to be a weak-pinning impurity, whereas titanium would be a strong-pinning impurity because it is nonisoelectronic. Lee and Rice[21] calculated that E_c varies as c^2 for isoelectronic impurities and c for nonisoelectronic impurities. We see that for the same resistance ratio of about 7.2, E_{c_2} is practically the same for tantalum or titanium impurities. We found that for different concentrations of titanium, tantalum, and zirconium impurities E_c increase with a law intermediate between c and c^2 without a difference in the type of impurities.[23]

As will be explained below we estimate that the different types of behavior near the critical field as observed in samples 1, 4, and 5 are due to the distribution of the pinning centers inside the crystal.

B. Noise

The variation of the rectified ac voltage generated in the crystal as a function of the applied current is shown in Fig. 4. The same features are observed for the noise signal as for dV/dI. A very sharp increase in noise appears at the same electric field where a dip in dV/dI is observed. In Fig. 4 we show the large band (0—200 kHz) noise. At low current the noise is instrumental and typically 2 at 3 μV. The noise voltage is typically 10^{-3} of the dc voltage near the critical current. The noise

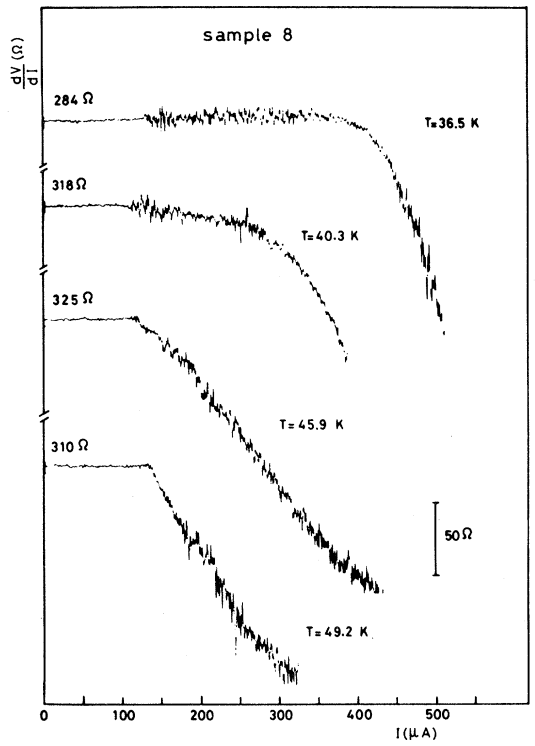

FIG. 3. Variation of the differential resistance dV/dI as a function of the applied current for $NbSe_3$ doped with titanium impurities (sample 8). The nominal amount of impurities is 1000 ppm. At low temperature it can be observed that low-frequency noise appears in a large electric field range before the decrease of dV/dI.

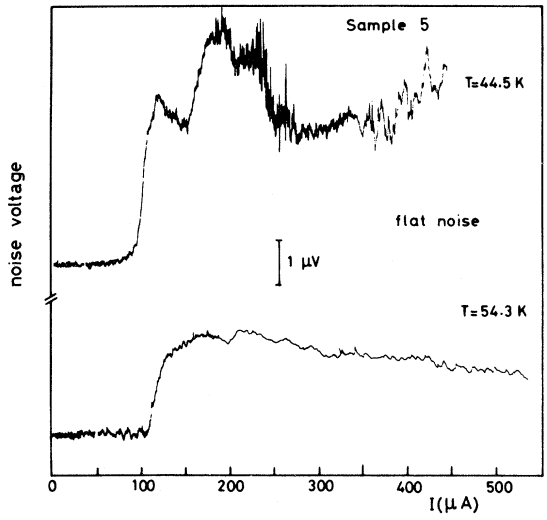

FIG. 4. Variation with the applied current of the broad-band noise voltage between the voltage leads of sample 5.

variation shows structures as first observed by Fleming and Grimes.[22] In paper II this signal will be analyzed with a spectrum analyzer and the study of the frequencies in the noise will be made.

C. Negative resistance

The extreme sensitivity on the temperature of the variation of dV/dI as a function of E is shown in Fig. 5 for sample 3. At 51 K dV/dI decreases smoothly above 500 μA with some rounding. Only 4 K lower, sample 3 shows the same behavior as does sample 5, i.e., a very sharp drop in dV/dI but more dramatically because the drop is larger than the nominal resistance of the sample at weak electric field. In the inset of Fig. 5 the $V(I)$ curve shows a "knee" with a nearly horizontal variation. This large dip urged us to see if a negative resistance might be observed in this sample. All the measurements in Figs. 1—5 were made with a regulated current with a source impedance much higher than the resistance of the sample. The negative resistance could be masked by parasite capacitances. We separated the sample from the copper sample holder by more than 3 mm of quartz to reduce these capacitances, but without effect on the dV/dI variation. We also shunted the current leads with capacitances between 2.2 nF and 2.2 μF to insure a voltage-controlled situation, but again the dV/dI variation was the same as for the current-controlled cases. In fact we tried to impose a current- or a voltage-controlled situation in a macroscopic scale, but the sample is formed by a network of domains, and for each domain neither the current nor the voltage is controlled and the overall behavior is not affected by extra capactiances.

D. Frequency dependence of the depinning field

As seen in Figs. 2, 3, and 5, a general feature of the variation of dV/dI at low temperature is the onset of noise at low frequency associated with a very small decrease of dV/dI in a large electric field range before the sharp drop of dV/dI. We have analyzed the frequency dependence of this noise with the PAR 124A lock-in amplifier used in ac mode with selected frequencies with a Q of 20. In Fig. 6 we show dV/dI at 24.3 K for sample 6. The variation is very similar to sample 3 although

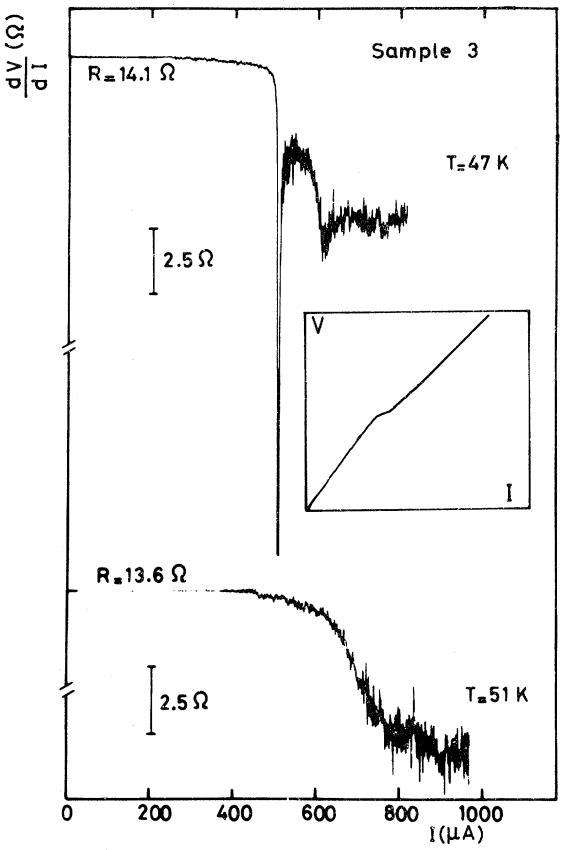

FIG. 5. Variation of the differential resistance dV/dI as a function of the applied current for sample 3. The drop in dV/dI is higher than the nominal resistance of the sample for very small current: In the inset the characteristic $V(I)$ is drawn. However, negative resistance was not observed in $NbSe_3$.

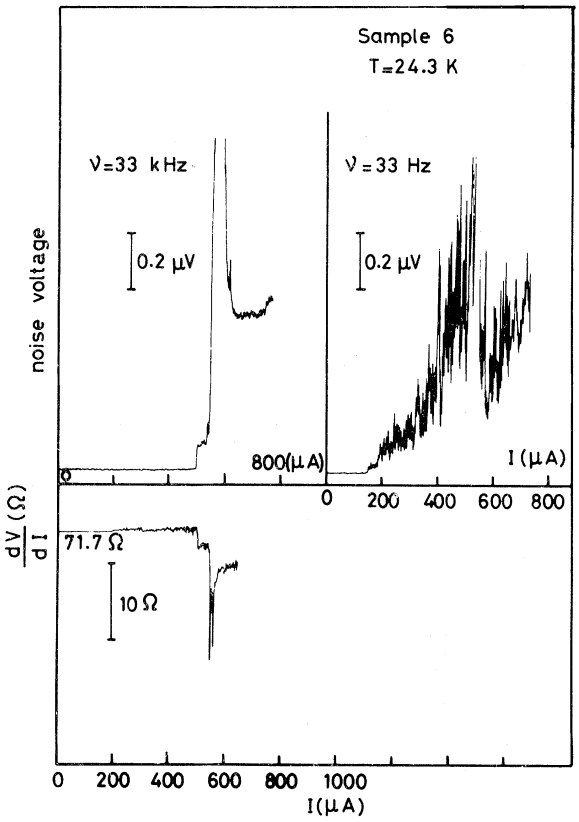

FIG. 6. In the lower part: variation of the differential resistance as a function of the applied current for sample 6. In the upper part: the noise voltage at 33 Hz starts to increase at 180 μA and the noise voltage for 3.3 kHz at 500 μA at the same current where dV/dI drops.

the drop is smaller. At 33 Hz, which is the frequency of the ac bridge, the amplitude of noise increases sharply at 180 μA (exactly as observed in the variation of dV/dI with the ac bridge) and is maximum at 500 μA. At 33 kHz the amplitude of noise increases only at 500 μA, where dV/dI drops suddenly. Thus we demonstrate that the definition of the critical field might be ambiguous and is a function of the frequency. As seen later in paper II we will associate the low-frequency noise with the depinning of independent individual domains, whereas we will show the sharp drop corresponds to the synchronization between all the domains. We can define two electric fields, the first field when the low-frequency noise appears and the second field when dV/dI starts to decrease. We have observed that these two electric fields become increasingly separated when the temperature decreases and converge into an unique critical field near the temperature where the resistivity is maximum for the lower CDW. This low-frequency noise does not seem to have been observed previously by Fleming[29] because of the too high band pass of the amplifiers he used.

E. Effect of a superposed rf field

We have seen in Sec. III D that a large frequency spectrum is associated with the sharp drop in dV/dI. We have applied a rf field with a constant amplitude and looked at its effect on the variation of dV/dI. The results for two frequencies are shown in Fig. 7. A rf intensity at 50 MHz has no effect on the shape of the dV/dI variation, which is identical to the zero rf intensity case. However, with a rf intensity at 100 kHz two effects are visi-

ble: Firstly, the dc critical field is reduced; secondly, the drop in dV/dI is much more gradual and the minimum dV/dI is practically removed. We have performed the same kind of experiments with different amplitudes of the rf fields and different frequencies on sample 5. We have observed that at relatively low frequencies (less than 200 kHz) when the amplitude of the rf field is not too large (less than the dc value) the dc electric field is reduced to a value E_c' such that the sum of E_c' and the rms value of the amplitude of the rf field equals the dc critical field without the rf field. But at higher frequencies (more than 1 MHz) there is no longer any effect on the dc critical current. This combination between large-amplitude rf fields with variable frequencies and dc fields needs more work to be completely understood.

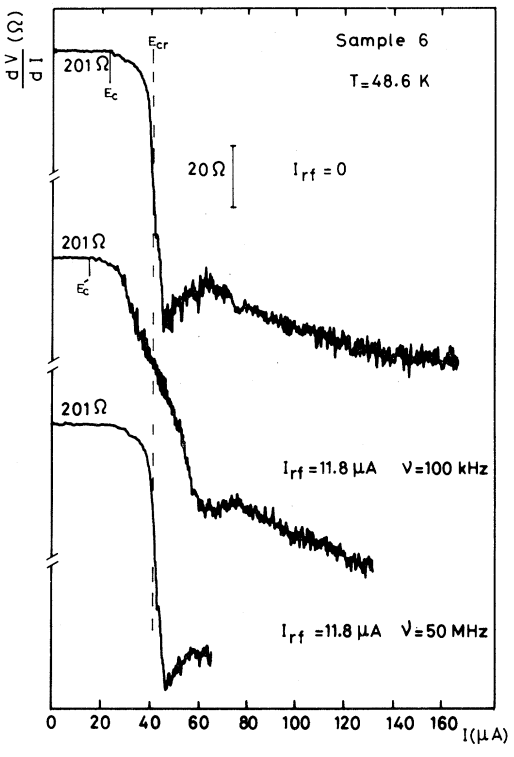

FIG. 7. Influence on the critical field of the superposition of a rf current on the dc current. At the frequency of 100 kHz the dc current is reduced compared to the value with zero-frequency current and the deep minimum in dV/dI is suppressed. At the frequency of 50 MHz the rf current has no effect on the dV/dI variation.

IV. PHENOMENOLOGICAL MODEL FOR CDW MOTION

The nonlinear transport properties of $NbSe_3$ are generally explained by the motion of the charge-density wave, which carries a net electrical current, superimposed on the current of free electrons when the field reaches a critical field, necessary to overcome pinning forces acting on the CDW condensate.

A. Physical hypothesis

We gave previously[32] the physical hypothesis of the model of CDW motion. We develop below in more detail the ingredients of such a model.

1. Charges in motion when CDW moves as a whole

If the wave vector $\vec{q}$ of CDW is incommensurate with the lattice and if the lattice-CDW interaction is not too strong, the position of the origin of phases for the CDW is degenerate, and we get a (Goldstone) degeneracy, i.e., a possible condensation in a moving frame with uniform speed v and with extra energy of inertial type. The effective mass m' of the CDW is a few electronic masses per condensed electron, due to a partial screening of the electric potential by a lattice deformation, so that ions get some oscillation kinetic energy in the case of motion of the CDW. If condensation were complete, i.e., for a true one-dimensional material at low temperature, the total current density associated with the motion of the CDW would be

$$j=-nev\ ,$$

where n is the total number of electrons in the band affected by the CDW per unit volume.

In the case of a strongly anisotropic metal like $NbSe_3$ the fit of the Fermi surface by a translation of $\vec{q}$ is probably not complete so that n is only an important fraction n' of the number of electrons in the band affected by the CDW condensation. Other parts of the Fermi surface give Ohmic conductivity in the CDW state at fields below the critical field. The total current density can now be written

$$j=-n'ev+\sigma E\ ,$$

where σ is the Ohmic conductivity at low electric fields.

2. *Forces acting on CDW*

There are three kinds of forces acting on CDW: electrical forces, damping forces, and pinning forces. We shall discuss these forces per unit volume.

Since the current carried by the velocity v is $-n'ev$, the electrical force is

$$F_{\text{el}} = -n'eE \ .$$

Damping forces may arise from various mechanisms: excitation of low-energy phasons by the motion, coupling of the oscillations of the lattice when the CDW moves with very-low-energy phonons by anharmonic terms, mutual friction between CDW and free-electron motions, etc. In any case the density of damping forces will be proportional to the velocity v, and at a given temperature can be defined by a coefficient of "viscosity":

$$F_{\text{damp}} = -\eta' v \ ,$$

with η' a function of T.

Pinning forces are more difficult to take in account. The main interaction between impurities and the phase of the CDW is via Friedel screening oscillations, which have an oscillatory behavior with $q = 2k_F$, the same as that for the CDW distortion. If the two oscillations have the same phase, they will help each other and we shall get a minimum in energy. For the opposite situation, phase opposition, the energy will be at a maximum. For a given position of the impurity r_i, we get a periodic energy, which can be written as

$$W_{\text{interact}} = -V_0 \cos[\phi(r_i) - \psi(r_i)] \ ,$$

where ϕ is the phase of the CDW at the impurity position, and ψ the ideal value taking into account the relative charge Z of the impurity in the matrix.

Just as with superconducting pinning, the main problem is how to sum these random forces to get a net irreversible force, which, at least for macroscopic samples, has to be proportional to the volume. Without further information we are reduced to working with hypothesis. The simplest one is the following.

At T_c, ξ is rather large, there is nucleation of CDW domains at places where in the random distribution of $\psi(r_i)$, and there is an overall coherent interaction which fixes the phase of the domain in an attractive position. At slightly lower temperatures the domains grow, encompassing less favorable ψ. When two domains arrive in contact, if the phase difference is small they give a single domain with well-defined phase, but if the phase difference is high enough (say of the order of π), a normal wall appears and subsists between the two adjacent independent domains.

This hypothesis is supported by the analogy with weak superconducting contacts giving the Josephson effect. In the case of superconductors, the amplitude and phase of the order parameter play the same role in the Ginzburg-Landau-Abrikosov-Gor'kov (GLAG) equation for free energy, but for a CDW distortion MacMillan[40] has shown that phasons have lower energy than amplitudons. However, our model is consistent with

(a) the observation by Fung and Steeds[33] of domains by electronic microscopy, and

(b) the appearance at low temperature of partial superconductivity observed by Haen *et al.*[41]

This last feature can be explained by the fact that it is well known that a one-dimensional material is ordered at low temperature, either by a CDW transition or a superconducting transition or a spin-density wave (SDW) transition. If by pressure one destroys the CDW transition T_2, $NbSe_3$ becomes a bulk superconductor with a critical temperature of 2.5 K.[7] However, at ambient pressure the CDW is suppressed in the surface of thickness ξ between two domains, and a filamentary superconductivity appears with nonzero resistivity and the absence of total Meissner effect.

The domains that we are discussing are not exactly the same as those postulated by Lee and Rice[21] for the weak-pinning impurities. In this case each impurity is too weak to pin the CDW, but the CDW can be pinned by the fluctuations of the number of impurities in a large volume. Each domain has a huge charge which consequently gives a very weak electric field to depin the wave. The main hypothesis of our domain description is that the order parameter is zero at the borders of each domain so that coupling between adjacent domains requires only conservation of the electric current and continuity of potential without any coupling, such as a Josephson potential.

Thus we think that the sample is formed by independent domains, each of them having a nearly ideal phase, in motion as

$$\phi(r,t) = qr + \phi_0(t)$$

and at equilibrium as

$$\phi = \vec{q}\cdot\vec{r} + \phi_0 \ .$$

Inside each domain, pinning forces can be expressed as

$$F = qV_0 \sum_i \sin[\phi_0 + (qr_i - \psi_i)]$$

where ϕ_0 is the phase, say, at the center of the domain. The composition of the random forces over (i) impurities belonging to the domain gives a net pinning force with a periodic dependence in ϕ_0:

$$F = F_0 \sin\phi_0 .$$

Since we have many domains each domain will be labeled by an index j:

$$F_{\text{pin}\,j} = +F_j \sin\phi_j ,$$

and the equation of motion will be

$$v_j(m'n'\vec{\gamma} + \eta'\vec{v} + n'e\vec{E}) - F_j \sin\phi_j = 0 , \tag{4a}$$

where v_j is the volume of the domain.

The velocity is associated with the translation of phase:

$$v = \frac{\partial\phi}{\partial t}\frac{1}{q} = \frac{d\phi_j}{dt}\frac{1}{q} .$$

Until frequencies are of the order of 10^{10}, the inertial term is much lower than the dissipative one, and one can use the equation of motion which is that of an overdamped oscillator:

$$\frac{\eta'}{q}\frac{\partial\phi_j}{\partial t} - \frac{F_j}{v_j}\sin\phi_j = -\eta' e\vec{E} . \tag{4b}$$

However, analysis of the properties of a CDW described by a damped oscillator including the inertial term has also been made.[42–44]

Since η' is not well defined by microscopic calculation, one can change η'/q to η, and by using the algebraic value of the electronic charge,

$$\eta\frac{\partial\phi_j}{\partial t} - f_j \sin\phi_j = \eta' eE .$$

f_j due to random composition of impurity potentials and phases has no reason to be the same for each domain. If, for example, a domain contains a mean value of 100 impurities, f_j is a random variable with a mean-square dispersion of $\frac{1}{10}$ of its mean value. Equation (4b) was recently derived by Grüner *et al.*[45] assuming the same hypothesis as that in Ref. 32.

B. Single-domain behavior

For a given domain we have two equations:

$$\eta\frac{\partial\phi}{\partial t} - f\sin\phi = \eta' eE , \tag{5a}$$

$$j = \eta' ev + \sigma E . \tag{5b}$$

The critical field is obtained for $d\phi/dt = 0$:

$$n'eE_c = f$$

and

$$E_c = \frac{f}{n'e} . \tag{6}$$

This electric field is the field when the electric force overcomes the pinning force. With the introduction of the dimensionless variable

$$\tau = \frac{\eta}{f} , \tag{7}$$

we can change Eq. (5a) to

$$\tau\frac{\partial\phi}{\partial t} - \sin\phi = \frac{E}{E_c} .$$

Equation (5b) can also be modified. If one applies a very high electric field $E >> E_c$, one experimentally can define β as

$$\beta = \frac{\sigma_{E\to\infty} - \sigma_{E\to 0}}{\sigma_{E\to 0}} . \tag{8}$$

In the equation of motion $\sin\phi$ is negligible compared to E/E_c,

$$\tau\frac{\partial\phi}{\partial t} \sim \frac{E}{E_c} ,$$

so that Eq. (5b) gives

$$j = \frac{n'e}{q}\frac{\partial\phi}{\partial t} + \sigma E = E\left[\sigma + \frac{n'e}{q\tau E_c}\right] ,$$

however,

$$\beta\sigma = \frac{n'e}{q\tau E_c} ,$$

and (5b) becomes

$$j = \sigma E + \beta\sigma\tau E_c\frac{\partial\phi}{\partial t} = \sigma\left[E + \beta E_c\tau\frac{\partial\phi}{\partial t}\right] .$$

Therefore (5a) and (5b) can be written as

$$\tau\frac{\partial\phi}{\partial t} = \frac{E}{E_c} + \sin\phi , \tag{9a}$$

$$j = \sigma\left[E + \beta E_c\tau\frac{\partial\phi}{\partial t}\right] . \tag{9b}$$

1. Behavior at a given field $E > E_c$

The phase ϕ increases by 2π after a period defined from (9a):

$$T=\tau\int_0^{2\pi}\frac{d\phi}{E/E_c+\sin\phi}$$
$$=2\pi\tau\frac{1}{[(E/E_c)^2-1]^{1/2}}\ .$$

The average value of $\partial\phi/\partial t$ is $\langle\partial\phi/\partial t\rangle_{\rm av}=2\pi/T$. Thus, above the critical field the motion is the superposition of a continuous drift and a modulation due to the pinning. The continuous current is, following (9b),

$$\bar{j}=\sigma[E+\beta(E^2-E_c^2)^{1/2}]\ , \tag{10}$$

and the modulation has periodic components with frequencies of a multiple of

$$\omega=\frac{1}{\tau}\left[\left[\frac{E}{E_c}\right]^2-1\right]^{1/2}\ . \tag{11}$$

The variation of ω with E indicates a curvature downwards, whereas experimentally the $\omega(E)$ variation is concave upwards.[32]

2. Behavior at a given current

E is now a function of time, but j is given and (9b) can be written

$$E=\frac{j}{\sigma}-\beta E_c\tau\frac{\partial\phi}{\partial t}\ ,$$

and (9a) can be written

$$\tau\frac{\partial\phi}{\partial t}=\left[\frac{j}{\sigma E_c}-\beta\tau\frac{\partial\phi}{\partial t}\right]+\sin\phi\ ,$$
$$\tau\frac{\partial\phi}{\partial t}(1+\beta)=\frac{j}{\sigma E_c}+\sin\phi\ .$$

The equation of motion is of the same as that in the case where E was imposed, but with a different time constant. Moreover,

$$\frac{j}{\sigma E_c}=\frac{j}{j_c}\ , \tag{12}$$

so that

$$T=2\pi\tau(1+\beta)\frac{1}{[(j/j_c)^2-1]^{1/2}}$$

and

$$\bar{E}=\frac{j}{\sigma}-\frac{\beta E_c}{1+\beta}\left[\left[\frac{j}{j_c}\right]^2-1\right]^{1/2}\ . \tag{13}$$

In Fig. 8 we have drawn the shapes of the characteristic $E(j)$ normalized to E_c and j_c in the two cases where the electric field [Eq. (10)] or the current [Eq. (13)] is regulated. In the same figure we have drawn the derivative dE/dj normalized to E_c and j_c for the two same cases. An important feature is that we get an infinitely negative differential resistance in the case of a current-regulated characteristic, and a zero differential resistance in the case of a field regulated near the critical conditions. For a very high electric field the limit value of dE/dj is $1/(1+\beta)$. It can be noted that the limit value is approached from lower values, whereas experimentally we find that dE/dj decreases towards this value for a very high electric field.

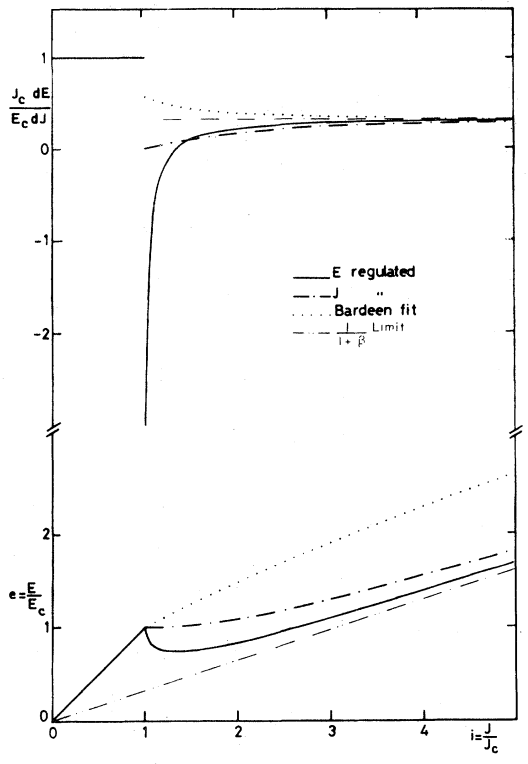

FIG. 8. Variation of $E(J)$ and dE/dJ normalized to E_c and j_c in the two cases where the electric field [Eq. (10)] or the current [Eq. (13)] is regulated. Also shown is the variation of $E(J)$ and dE/dJ obtained by Bardeen [Eq. (24)] in his theory of the tunneling of the CDW though the impurity pinning.

3. *Fourier components of the current at regulated field*

We shall write

$$\frac{E}{E_c}=e>1 .$$

Equation (9a) gives

$$\tau\frac{\partial\phi}{\partial t}=e+\sin\phi . \tag{9a'}$$

If ϕ is the solution of (9a'), the function

$$z=\frac{1}{e+\sin\phi} \tag{14}$$

is a function of time which obeys the differential equation

$$\frac{\tau^2}{e^2-1}z''+z=\frac{e}{e^2-1} ,$$

as can be seen by two time derivatives, so that

$$z=\frac{1}{e^2-1}\left[e+\sin\left[\frac{(e^2-1)^{1/2}}{\tau}t+\psi\right]\right] , \tag{15}$$

where ψ is an arbitrary phase factor. However, we have

$$\frac{d\phi}{dt}=\frac{1}{\tau}(e+\sin\phi)=\frac{1}{\tau}\frac{1}{z} ,$$

so

$$\tau\frac{d\phi}{dt}=(e^2-1)\frac{1}{e+\sin(\omega t+\psi)} ,$$

where we have written

$$\omega=\frac{(e^2-1)^{1/2}}{\tau} . \tag{11'}$$

Standard Fourier-transform calculation gives

$$\tau\frac{d\phi}{dt}=(e^2-1)^{1/2}\left[1+2K\cos\left[\omega t+\frac{\pi}{2}+\psi\right]+2K^2\cos 2\left[\omega t+\frac{\pi}{2}+\psi\right]+\cdots\right.$$
$$\left.+2K^n\cos n\left[\omega t+\frac{\pi}{2}+\psi\right]+\cdots\right] , \tag{16}$$

with

$$K=e-(e^2-1)^{1/2} . \tag{17}$$

The amplitude of the fundamental frequency is simply

$$2(e^2-1)^{1/2}[e-(e^2-1)^{1/2}$$

From (9b) the current carried by the CDW is

$$j_{\mathrm{CDW}}=\sigma\beta E_c\tau\frac{\partial\phi}{\partial t} , \tag{18}$$

and $\tau\partial\phi/\partial t$ is given by Eq. (16).

In Fig. 9 we have plotted the amplitude of the different components to j_{CDW} normalized to j_c as a function of the normalized electric field E/E_c. The amplitude of the fundamental frequency tends to a finite value

$$j_\omega=\sigma\beta E_c \quad \text{for } E>>E_c ,$$

but the relative amplitude of the high-level harmonics decreases rapidly when e is above 1.5. In this model high-level harmonics only near the critical field have a sufficient amplitude to be observed.

Although we measure in some cases a sharp drop in dV/dI, the nonobservation of negative differential resistance of E_c leads us to think that a model with an unique domain is not very realistic and that we must consider the sample as formed with many domains.

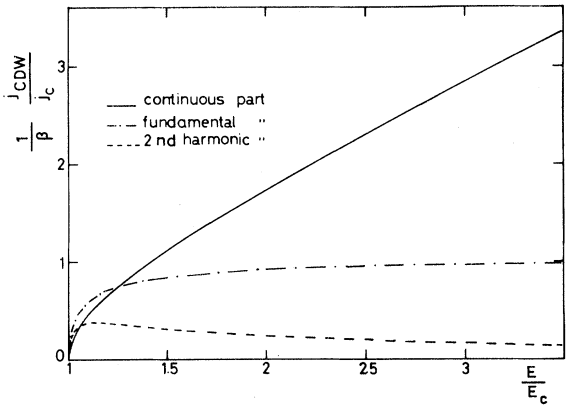

FIG. 9. Variation as a function of the normalized electric field of the continuous current and of the fundamental and second-harmonic periodic components of the current carried by the CDW.

C. Multidomain behavior

As we shall see later, when we consider many independent domains, we generally have problems arising by a linking in phase of the oscillations of a great number of them. Here we only consider a statistical distribution of domains, each one working independently of the others, *in a mean-field approximation.*

Let us call $p(E_c)dE_c$ the normalized probability to observe a domain with a critical field in the range E_c, E_c+dE_c. E_M is the mean value of this law and s its standard deviation.

As noticed in Sec. III C, neither field nor current are imposed for a given domain. However, in the thermodynamic limit, macroscopic mean values of fields and currents can be determined.

For a given macroscopic applied field E, any domain with

$$E_c < E \ ,$$

will be depinned. We can apply a first-order approximation equivalent to a mean-field theory in magnetism by noting that the local density of current and the local electric field behave like microscopic induction and field in a magnetic material:

$$\vec{\nabla}\cdot\vec{j}=0, \quad \vec{\nabla}\cdot\vec{B}=0 \ , \tag{19a}$$

$$\vec{\nabla}\times\vec{E}=0, \quad \vec{\nabla}\times\vec{H}=0 \ , \tag{19b}$$

$$j=\sigma\left[E+\beta\tau\frac{\partial\phi}{\partial t}\right], \quad B=\mu_0(H+J) \ . \tag{19c}$$

Therefore the Ohmic conductivity appears equivalent to the vacuum permittivity μ_0, and the motion of the phase in the depinned domains acts like a magnetization. To first order we can replace interactions between domains by defining a hole in which the considered domain is placed, so that it experiences the mean field calculated by demagnetizing coefficients using the macroscopic mean values of H and B, i.e., $\bar{E}$ and $\bar{j}$.

Since observed domains are highly elongated cylinders,[33] demagnetizing coefficients can be neglected, and the mean field on each domain is equal to the mean macroscopic field. Each depinned domain gives an extra current:

$$\delta j_c=\sigma\beta E_c\left[\left(\frac{E}{E_c}\right)^2-1\right]^{1/2} .$$

Hence the extra mean continuous current $\overline{\delta j}$ in the sample in the applied field E is:

$$\overline{\delta j}=\sigma\beta\int_0^E p(E_c)(E^2-E_c^2)^{1/2}dE_c \ . \tag{20}$$

By differentiation we obtain the extra conductance:

$$\frac{d\overline{\delta j}}{dE}=\sigma\beta E\int_0^E\frac{P(E_c)dE_c}{(E^2-E_c^2)^{1/2}} \ . \tag{21}$$

This integral is always convergent and gives a finite value of the extraconductance, contrary to an infinite value in the case of a single domain.

In Fig. 10 we have plotted $\sigma dE/dj$ as a function of E/E_M for several values of s/E_M with a Gaussian distribution for $p(E_c)$. If the Gaussian distribution is very sharp (for small s/E_M) a very sharp macroscopic variation of the differential conductance of the sample is found, in reasonable agreement with the experiment critical field. For a large distribution it becomes very difficult to define a critical field.

D. Noise

With the same approximations we can account for the noise. Each domain works independently of the others with an arbitrary phase but at a well-defined frequency. At any field we have a whole spectrum of noise, starting from zero frequency, for the domains which are just depinned for E, to high frequency, for the domains which have a very small critical field compared to E. However, in reality the number of oscillators decreases drastically when we reach an E_c which is a few s below E_M. Since one expects that s is much smaller (say $\frac{1}{10}$ or less) than E_M and that E_M is of the order of the macroscopic critical field for the

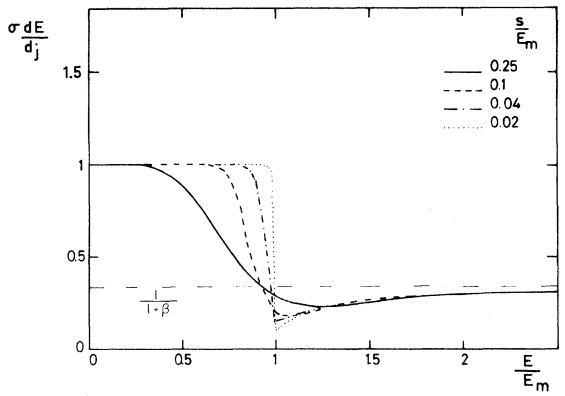

FIG. 10. Effect of a Gaussian distribution (E_M maximum value, s = standard deviation) on the discontinuity of dE/dJ at E_c. With large s/E_M values no definition of a critical field is possible.

sample, noise can be considered as vanishingly small for applied electric fields less than $0.7E_M$.

The effective current for a given domain (k) is obtained by squaring and summing the Fourier components of Eq. (16):

$$\langle j_k^2 \rangle = (\sigma\beta E_c)^2(e^2-1)\frac{2K^2}{1-K^2} = (\sigma\beta E_c)^2 g\left[\frac{E}{E_c}\right] . \quad (22)$$

using the value of K [Eq. (17)], one finds the following curve (Fig. 11) for the numerical factor g. Just as for the distribution of excess continuous current, the formula giving the total broad band noise is

$$\langle j^2 \rangle = (\sigma\beta)^2 \int_0^E p(E_c)dE_c E_c^2 g\left[\frac{E}{E_c}\right] . \quad (23)$$

If one considers the applied low-field limit, say below $E_M - s$, due to the large variation of $p(E_c)$ the only important part of the integrals [Eq. (20)] or $\langle j^2 \rangle$ [Eq. (23)] is the immediate vicinity of E, where the factors $(E^2-E_c^2)$ and g have the same kind of variation, so that the broad-band noise becomes important for the same fields for which dV/dI shows deviations from an Ohmic behavior. The fact that in some cases noise appears before any detectable variation of dV/dI can be measured may be due to the better sensitivity of noise measurements but perhaps also to the crudeness of "the molecular field" approximation for transport phenomena.

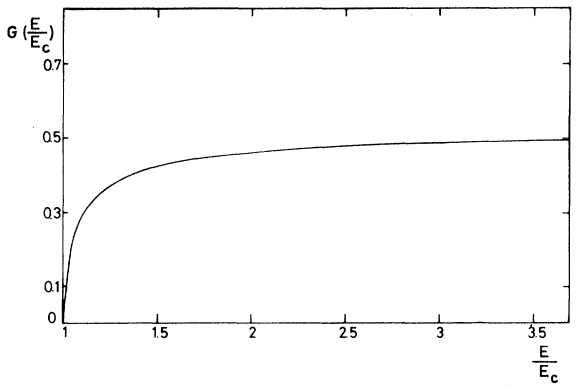

FIG. 11. Variation with the normalized electric field of the numerical factor $g=(e^2-1)2K^2/(1-K^2)$ which is used for calculating the broad-band noise for a multiple-domain sample.

E. Superposed rf fields

If one applies a non-negligible rf field $E_0\cos\omega_0 t$, superposed on a dc field less than E_c, it is interesting to discuss what can happen if

$$E_0 + E_{dc} > E_c .$$

During a fraction of the period corresponding to ω_0, the total field will exceed the critical field.

If $\omega_0\tau << 1$, the time during which the applied field exceeds the critical field is long compared to the eigenfrequency, and the phase has enough time to drift over several periods, giving an extra dc component even if $E_{dc} < E_c$.

In contrast if $\omega_0\tau >> 1$, the phase does not have enough time to change the value of the $\sin\phi$ component, and there is no contribution to the dc conductivity. This qualitative description agrees relatively well with the results shown in Fig. 7 and described in Sec. III E.

V. DISCUSSION AND CONCLUSIONS

The results obtained in Sec. IV B are essentially the mathematical formulation of the model we have developed previously to explain the quasi-periodical noise.[32] Several expressions for the conductivity associated with the motion of the CDW have been derived. Besides the empirical expressions of Fleming [Eqs. (1) and (2)], the expression obtained with our model [Eq. (18)], and that obtained by Grüner *et al.*,[45] the extra conductivity was calculated by Bardeen[28] in his theory of tunneling of the CDW through the pinning centers. With the introduction of a correlation length, he found.

$$\sigma = \begin{cases} \sigma_a \text{ for } E < E_c \\ \sigma_a + \sigma_b P(x) \end{cases} \quad (24)$$

with $P(x)=(1-1/x)e^{-1/x}$ and $x=E/E_c$.

In Fig. 8 we have plotted dE/dj following Eq. (24). We see that at the critical field dE/dj normalized to E_c and j_c has a discontinuity between 1 and $2.73/(2.73+\beta)$ and that after this drop dE/dj decreases exponentially to its limit value $1/(1+\beta)$. Equation (24) requires a unique correlation length, but the same generalization as that in Sec. IV C with a Gaussian distribution of correlation lengths can be made which, similar to the curves shown in Fig. 11, will suppress the sharp drop in dE/dj at E_c. However, the Bardeen model gives at high electric field a decreasing dE/dj towards its limit

value, in agreement with the experimental results.

Temperature dependences of the critical fields have been measured for the two CDW's. E_c is minimum in the temperature range where the resistivity of $NbSe_3$ shows a maximum at $T=123$ K for the upper transition and $T=47$ K for the lower transition. E_c diverges when T reaches the critical temperatures T_1 and T_2, but also increases sharply below 123 and 47 K. The divergence near T_c can be easily understood because the number of condensed electrons below the CDW gap is small, and following [Eq. (6)] the critical field varies as $1/n'e$. However, for temperatures in the order of 123 and 47 K the CDW gaps are well developed, and $n'e$ must be constant. The increase of E_c at low temperature must be explained by an increase of the pinning force per unit volume. The origin of such an increase is not very clear but might come from a fragmentation of the CDW lattice into smaller domains.

To account for the shape of the dV/dI variation for a given sample, consideration of the critical field distribution with temperature must be made. For samples 1 and 4 we can expect that in these relatively pure samples the Gaussian distribution of critical field is large enough to suppress the sharp drop in dV/dI. This is the case also for doped samples where the rounding of dV/dI near E_c indicates a rather inhomogeneous distribution of domains. But for samples 3,6, etc., it must be assumed that the width of the Gaussian distribution varies with temperature, and that below approximately 45 K all the domains are almost identical giving a narrow distribution of critical fields and consequently leading to the observation of a sharp dip in dV/dI. We want to point out that Fleming has not measured any jumps in dV/dI of very pure samples (resistance ratio around 200) as we have shown. Also, to conclude this work in the study of the dV/dI characteristics of $NbSe_3$ we think that the important parameter for the shape dV/dI near the critical field is not essentially the purity of the sample but the repartition of the pinning centers. As in the case of superconductors, studies with a periodic pinning would be important to clarify the rather complicated experimental situation.

[1]A. Meerschaut and J. Rouxel, J. Less-Common Met. 39, 197 (1975).
[2]P. Haen, P. Monceau, B. Tissier, G. Waysand, A. Meerschaut, P. Molinié, and J. Rouxel, in *Proceedings of the Fourteenth International Conference on Low Temperature Physics, Otaniemi, Finland, 1975,* edited by M. Krusius and M. Vuorio (North-Holland, Amsterdam, 1975), Vol. 5, p. 445.
[3]K. Tsutsumi, T. Tagagaki, M. Yamamoto, Y. Shiozaki, M. Ido, T. Sambongi, K. Yamaya, and Y. Abe, Phys. Rev. Lett. 39, 1675 (1977).
[4]J. L. Hodeau, M. Marezio, C. Roucau, R. Ayrolles, A. Meerschaut, J. Rouxel, and P. Monceau, J. Phys. C 11, 4117 (1978).
[5]C. Roucau, R. Ayrolles, P. Monceau, L. Guemas, A. Meerschaut, and J. Rouxel, Phys. Status Solidi A 62, 483 (1980).
[6]R. M. Fleming, D. E. Moncton, and D. B. McWhan, Phys. Rev. B 18, 5560 (1978).
[7]P. Monceau, J. Peyrard, J. Richard, and P. Molinié, Phys. Rev. Lett. 39, 160 (1977).
[8]A. Briggs, P. Monceau, M. Nunez-Regueiro, J. Peyrard, M. Ribault, and J. Richard, J. Phys. C 13, 2117 (1980).
[9]A. Briggs, P. Monceau, M. Nunez-Regueiro, M. Ribault, and J. Richard, J. Phys. (Paris) 42, 1453 (1981).
[10]W. W. Fuller, Ph.D. thesis, University of California at Los Angeles, 1980 (unpublished); W. W. Fuller, G. Grüner, P. M. Chaikin, and N. P. Ong, Chem Scr. 17, 205 (1981).
[11]K. Nishida, T. Sambongi, and M. Ido, J. Phys. Soc. Jpn. 48, 331 (1980).
[12]W. W. Fuller, P. M. Chaikin, and N. P. Ong, Solid State Commun. 30, 689 (1979).
[13]P. Monceau, Solid State Commun. 24, 331 (1977); P. Monceau and A. Briggs, J. Phys. C 11, L465 (1978).
[14]R. Fleming, J. A. Polo, and R. V. Coleman, Phys. Rev. B 17, 1634 (1978).
[15]P. Monceau, N. P. Ong, A. M. Portis, A. Meerschaut, and J. Rouxel, Phys. Rev. Lett. 37, 602 (1976).
[16]N. P. Ong and P. Monceau, Phys. Rev. B 16, 3443 (1977).
[17]G. Grüner, L. C. Tippie, J. Sanny, W. G. Clark, and N. P. Ong, Phys. Rev. Lett. 45, 935 (1980).
[18]J. Bardeen, in *Highly Conducting One Dimensional Solids,* edited by J. T. Devreese (Plenum, New York, 1979), p. 373.
[19]H. Fröhlich, Proc. R. Soc. London Ser. A 223, 296 (1954).
[20]P. A. Lee, T. M. Rice, and P. W. Anderson, Solid State Commun. 14, 703 (1974).
[21]P. A. Lee and T. M. Rice, Phys. Rev. B 19, 3970 (1979).
[22]R. Fleming and C. C. Grimes, Phys. Rev. Lett. 42,

1423 (1979).
[23]P. Monceau and J. Richard (unpublished).
[24]N. P. Ong, J. W. Brill, J. C. Exkert, J. W. Savage, S. K. Khanna, and R. B. Somoano, Phys. Rev. Lett. 42, 811 (1979); Phys. Rev. B 23, 1517 (1981).
[25]K. Maki, Phys. Rev. Lett. 39, 46 (1977).
[26]J. B. Sokoloff, Phys. Rev. B 23, 1992 (1981).
[27]J. Bardeen, Phys. Rev. Lett. 42, 1498 (1979).
[28]J. Bardeen, Phys. Rev. Lett. 45, 1978 (1980).
[29]R. Fleming, Phys. Rev. B 22, 5606 (1980).
[30]M. Weger, G. Grüner, and W. G. Clark, Solid State Commun. 35, 243 (1980).
[31]N. P. Ong and C. M. Gould, Solid State Commun. 37, 25 (1981).
[32]P. Monceau, J. Richard, and J. Renard, Phys. Rev. Lett. 45, 43 (1980).
[33]K. K. Fung and J. W. Steeds, Phys. Rev. Lett. 45, 1696 (1980).
[34]D. W. Bullett, J. Phys. C 12, 277 (1979); Solid State Commun. 26, 563 (1978).
[35]R. Hoffman, S. Shaik, J. S. Scott, M.-H. Whangbo, and M. J. Foshee, J. Solid State Chem. 34, 263 (1980).
[36]J. A. Wilson, Phys. Rev. B 19, 6546 (1979).
[37]S. Nakamura and R. Aoki, Solid State Commun. 27, 151 (1978).
[38]H. Kahlert, private communication.
[39]G. X. Tessema and N. P. Ong Phys. Rev. B 23, 5607 (1981).
[40]W. L. McMillan, Phys. Rev. B 12, 1197 (1975).
[41]P. Haen, J. M. Mignot, P. Monceau, and M. Nunez-Regueiro, J. Phys. (Paris) Colloq. 39, C6-703 (1978).
[42]M. J. Rice, S. Strassler, and W. R. Scheider, in *One-dimensional Conductors,* Vol. 34 of *Lecture Notes in Physics,* edited by H. G. Schuster (Springer, Berlin, 1975), p. 282.
[43]W. Wonneberger, in *Quasi-one-dimensional Conductors,* Vol. 95 of *Lecture Notes in Physics,* edited by S. Barišic, A. Bjeliš, J. R. Cooper, and B. Leontić (Springer, Berlin, 1979), p. 311.
[44]M. Papoular, Phys. Lett. 76A, 430 (1980).
[45]G. Grüner, A. Zawadowski, and P. M. Chaikin, Phys. Rev. Lett. 46, 511 (1981).